Induced Liquid Crystalline Diversity in Molecular and Polymeric Charge-Transfer Complexes of Discotic Mesogens

Paul H. J. Kouwer,† Otto van den Berg, Wolter F. Jager, Wim J. Mijs, and Stephen J. Picken*

Delft University of Technology, Polymer Materials and Engineering, Julianalaan 136, 2628 BL Delft, The Netherlands

Received September 13, 2001; Revised Manuscript Received December 27, 2001

ABSTRACT: Charge-transfer complexes of a disk-shaped electron-rich donor, based on pentakis-(phenylethynyl)phenol and a series of electron-deficient acceptors, based on 2,4,7-trinitro-9-fluorenone have been prepared. Specific interactions resulted in supramolecular assemblies that exhibited various mesophases, although none of the pure materials showed liquid crystalline properties. Complexes of the low molar mass donor with a weak, intermediate, and a strong acceptor exhibited N_D, N_{Col}, and Col_h phases, respectively, as well as strong increases in the melting and clearing temperatures. Complexes with the corresponding macromolecular donor showed the nematic lateral (N_L) phase. In addition, suppression of crystallization led to mesophases stable over a wide temperature range. The use of a polymer bound mesogens and charge-transfer complexing are effective tools to induce a wide variety of unusual mesophases, starting from a limited number of materials.

Introduction

Since their discovery in the late 1970s,[1] discotic liquid crystals (DLCs) have received growing attention. A wide range of flat and rigid molecules, usually substituted by multiple flexible tails, have been synthesized and investigated for their liquid crystalline properties.[2] To take advantage of macromolecular properties, the mesogens were functionalized and incorporated into main chain[3a−e] and side chain polymers[3d−j] as well as in polymer networks.[3j−l] Recently, we reported for some discotic polymers an increased diversity in the liquid crystalline phase behavior; i.e., mesophases were found in high molar mass materials that were not observed in their corresponding low molar mass analogues.[3i,4] Another advantage of macromolecules is that in general crystallization is suppressed, and hence, a broad temperature window for the mesophases can be obtained. In addition, a desired liquid crystalline texture can be frozen in below the glass transition temperature or stored permanently by means of a cross-linking process in the mesophase.

Discotic liquid crystals can self-organize into various mesophases (see Figure 1). Two nematic phases are well-established. In the nematic discotic (N_D) phase, which was reported just after the discovery of discotic liquid crystals,[5] the molecules only possess orientational order. The nematic columnar (N_{Col}) phase, described 10 years later,[3d,6] is characterized by a columnar stacking of the molecules and a nematic arrangement of the aggregated columns. Recently, we reported a third nematic phase, where the disk-shaped molecules aggregate into large disk-shaped superstructures, and these aggregates show a nematic arrangement. The phase is referred to as the nematic lateral (N_L) phase due to the strong lateral interactions.[5c] Note that for the superstructures of the N_L and the N_{Col} phase the local organization can be very high, but the long-range positional order is very low, i.e., nematic. Besides the three nematic phases, several columnar phases are known for disk-shaped mesogens. In a columnar phase, the molecules are stacked into columns, which exhibit a long-range two-dimensional arrangement. Examples are the columnar hexagonal (Col_h) phase or columnar (ortho)rhombic phases (the latter not shown).

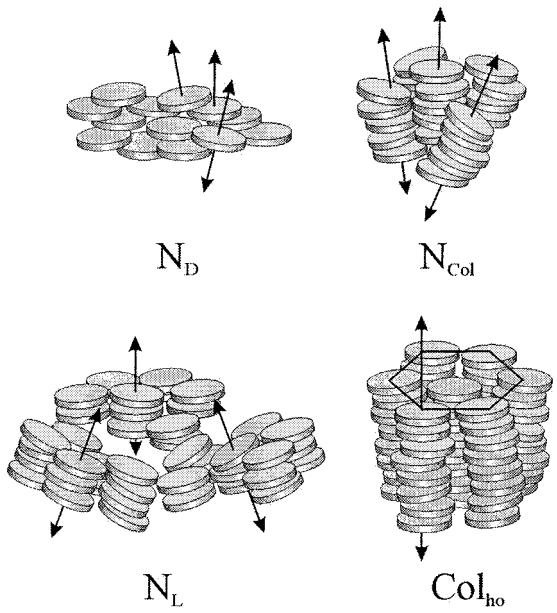

Figure 1. Common discotic mesophases: N_D = nematic discotic, N_{Col} = nematic columnar, N_L = nematic lateral, and Col_h = columnar hexagonal. Note that the extent of aggregation can be much larger than indicated in the picture.

Specific inter- and intramolecular interactions, like ionic, H-bond, and charge transfer (CT) interactions, can play a crucial role in the phase formation of liquid crystals. Discotic mesogens are particularly suitable to induce CT interactions.[7] The disk-shaped molecules generally have an extended aromatic core, and with the appropriate substituents, they can act as electron-rich "donors" when complexed with planar electron-deficient molecules. Commonly, 2,4,7-trinitro-9-fluorenone (TNF) or its derivatives are used, but other nitro-, cyano-, or

† Current address: Department of Chemistry, University of Hull, Cottingham Road, Hull, HU6 7RX, United Kingdom.
* Author for correspondence. E-mail: S.J.Picken@tnw.tudelft.nl.

10.1021/ma011628c CCC: $22.00
Published on Web 02/22/2002

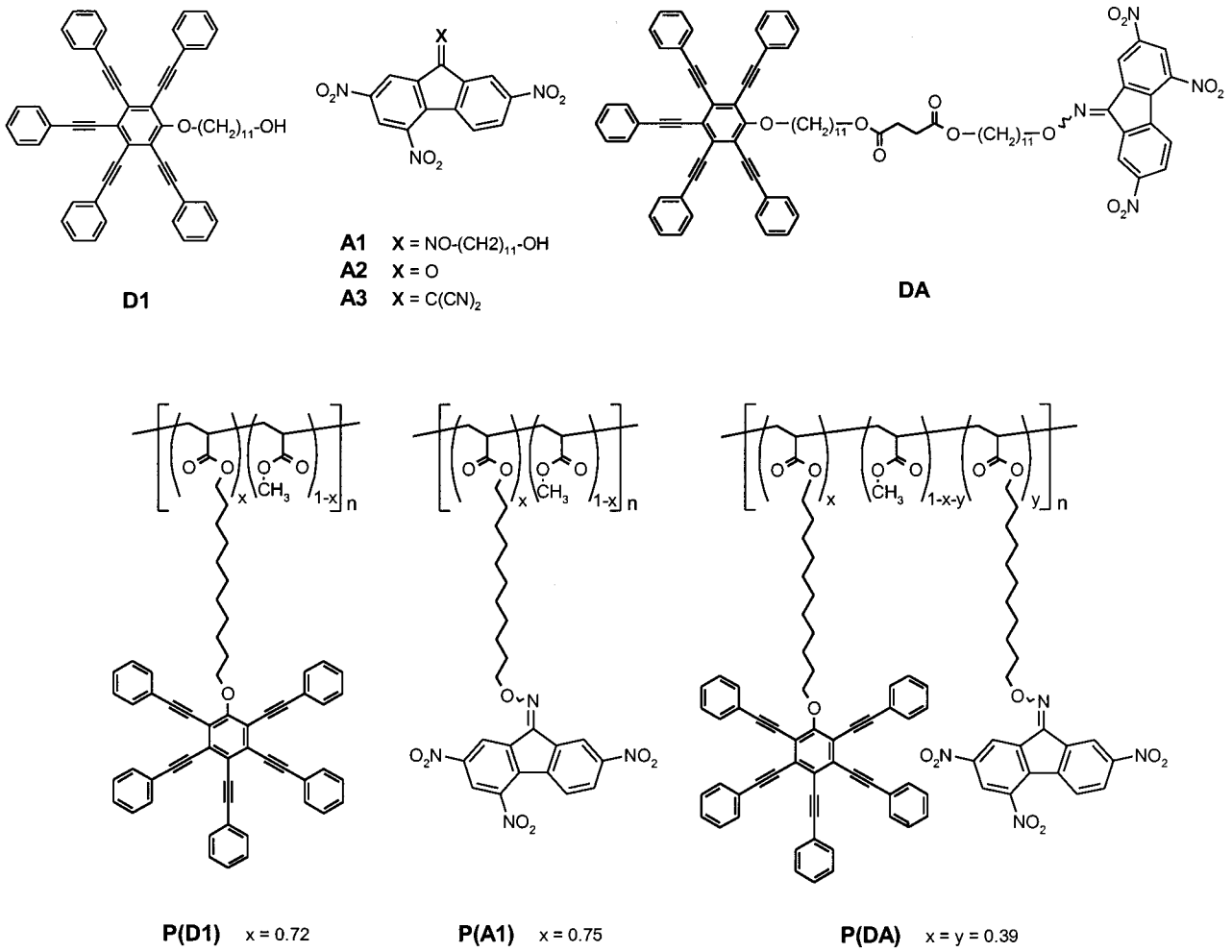

Figure 2. Studied materials.

fluoro-substituted arenes have been employed as well. By CT interactions, mesophases can be induced (via complexing of two nonliquid crystalline compounds), modified (another mesophase appears), or stabilized (by extending of the temperature window of mesophase formation).

Here, we report the properties of CT complexes of the disk-shaped materials: low molar mass **D1** and polymer **P(D1)** with a series of TNF-based electron acceptors; low molar mass **A1**−**A3** and polymer **P(A1)** (see Figure 2). Polymers **P(D1)** and **P(A1)** and copolymer **P(DA)** were synthesized by a straightforward esterification reaction of poly(acryloyl chloride). The properties of these materials and their CT complexes were investigated by optical polarizing microscopy (OPM), differential scanning calorimetry (DSC), and powder X-ray diffraction (XRD). The induced mesophases, found in all equimolar CT complexes, were analyzed, and the advantages of using polymeric species are clearly demonstrated.

Experimental Section

Materials. All materials were used as purchased without further purification unless mentioned otherwise. Pyridine was distilled from CaH_2 and CH_2Cl_2 from P_2O_5. The mesogen[8] **4** and poly(acryloyl chloride)[3i] (PAC) were prepared according to literature procedures. The crude polymerization mixture of PAC (M_n = 3000 g mol^{-1}, PDI = 2.9) was stored in a refrigerator and used without further purification.

Instrumentation. Nuclear magnetic resonance (NMR) spectra were taken on a Varian VXR 300 or VXR 400 MHz spectrometer. Chemical shifts are reported in ppm relative to TMS. Molecular weights were determined by gel permeation chromatography (GPC) in THF against narrow polystyrene standards. The thermal properties of the materials were investigated by a Perkin-Elmer DSC 7 differential scanning calorimeter (in nitrogen atmosphere) and a Jenapol optical polarizing microscope, equipped with a Mettler FP82 HT hot stage and a Mettler FP80 central processor. The mesophases of the complexes were studied with XRD analysis, using a Siemens Kristalloflex 710D X-ray generator with graphite monochromated Cu Kα radiation (λ = 1.54 Å), equipped with a Bruker HI-STAR area detector. The samples were oriented in a magnetic field using a Supper SmCo permanent magnet with a field of about 1.5 T and a custom-built capillary heating element.

Poly[11-(pentakis(phenylethynyl)phenoxy))undecyl acrylate-*co*-methyl acrylate] (P(D1)). A solution of the mesogen **D1** (1.0 g, 1.31 mmol), pyridine (1 mL), and 4-(*N*,*N*-dimethylamino)pyridine (DMAP) (catalytic amount) in freshly distilled CH_2Cl_2 (20 mL) was flushed with argon. The crude polymer solution (83 mg of polymer, 9.2 mmol of acyl groups) was added via a syringe. The mixture was stirred for 24 h at room temperature. To convert any remaining acyl groups, dry methanol (2 mL) was added. After 3 h, the mixture was precipitated in dry methanol, filtered, and reprecipitated from CH_2Cl_2 into methanol. After filtration and drying, the polymer was obtained as a pale yellow powder. The degree of substitution as calculated from peak integrations of the ^{1}H NMR spectrum was found to be 78%. Yield: 0.98 mg, 89% based on mesogen conversion. All peaks broadened significantly, so that no peak splitting was detected. ^{1}H NMR ($CDCl_3$): δ 7.6−7.2 (CH aromatic); 4.0 (CH_2OPh) 4.3 (CO_2CH_2); 3.6 (CH_3 methyl acrylate); 2.5−1.1 (CH_2, CH aliphatic spacer and backbone).

Scheme 1

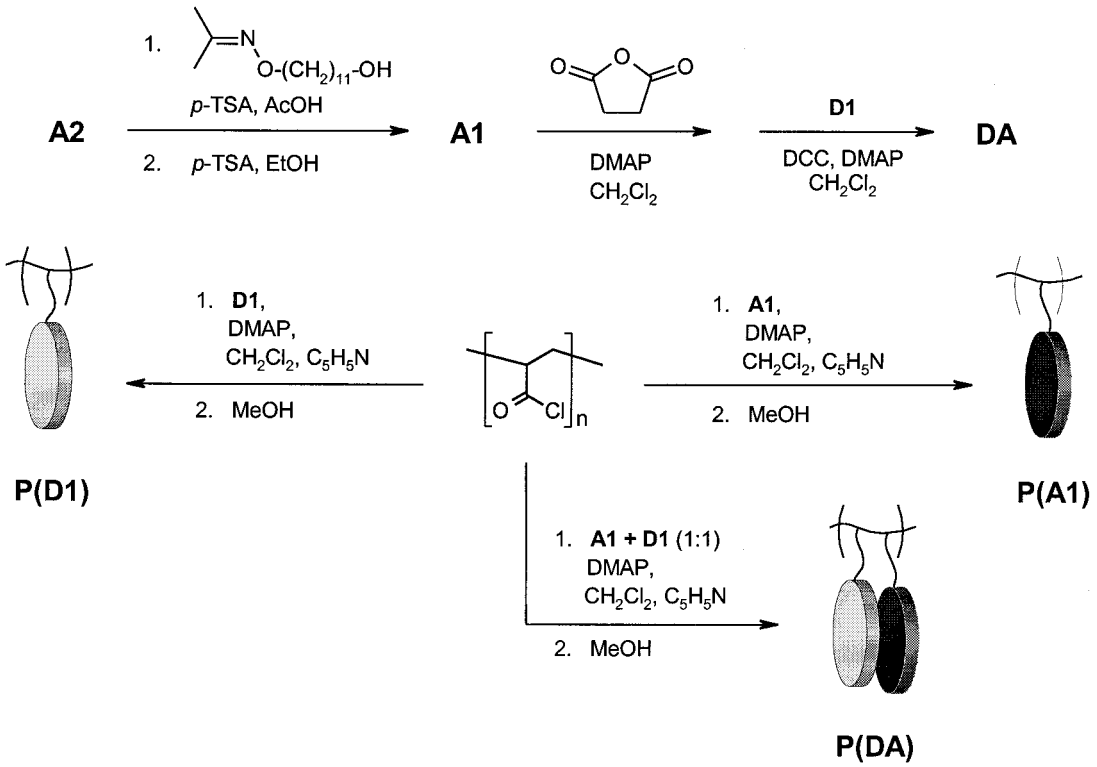

((*Z*,*E*)-2,4,7-Trinitro-9-fluorenylideneaminooxy)undecan-11-ol (A1). A solution of 2,4,7-trinitro-9-fluorenone (**A2**) (1.0 g, 3.2 mmol) and propane-2-one-*O*-(11-hydroxyundecyl)-oxim (1.5 g, 6 mmol) and *p*-toluenesulfonic acid (catalytic amount) were refluxed in glacial acetic (25 mL) until TLC indicated complete conversion. Water (25 mL) was added to the cooled reaction mixture, and the crude product (acetylated **A1**) was obtained by filtration, washed with water, and dried. Acetylated **A1** and *p*-toluenesulfonic acid (catalytic amount) were refluxed in ethanol (50 mL) for 16 h. Water (200 mL) was added to the cooled solution, and the crystallized product was filtered, washed with water, and dried. Pure **A1** was obtained after column chromatography (SiO_2, eluent: toluene to toluene:acetone 95:5), yielding pale yellow crystals (1.16 g, 73%). ^{1}H NMR (300 MHz, $CDCl_3$): δ 9.45−8.20 (m of *E*/*Z* isomers, 5H); 4.63 (t, 2H, CH_2ON); 3.64 (t, 2H, CH_2OH); 1.96, 1.95, 1.60−1.20 (m, 9 × 2H, spacer).^{13}C NMR (300 MHz, $CDCl_3$): δ 116.8−149.4 (25 × s fluorene, due to *E*/*Z* isomers); 78.5 (CH_2ON); 63.0 (CH_2OH); 25.7−32.8 (9 × s spacer).

Poly[11-((*Z*,*E*)-2,4,7-trinitro-9-fluorenylideneaminooxy)undecyl acrylate-*co*-methyl acrylate] (P(A1)). The polymer was prepared from **A1** and PAC as described for **P(D1)**. For the second precipitation of the polymer, hot ethanol was used, yielding the product as a pale yellow powder with a degree of substitution of 77% in a yield of 70%. All peaks broadened significantly, so that no peak splitting was detected. ^{1}H NMR ($CDCl_3$): δ 9.3−7.9 (CH aromatic fluorene); 4.6 (CH_2-ON); 4.0 (CO_2CH_2); 3.6 (OCH_3 methyl acrylate); 1.0−2.4 (CH_2, CH aliphatic spacer and backbone).

Succinic Acid 11-[Pentakis(phenylethynyl)phenoxy]-undecyl Ester 11-(2,4,7-Trinitro-9-fluorenylideneaminooxy)undecyl Ester (DA). A solution of **A1** (1.0 g, 2.0 mmol), succinic anhydride (0.40 g, 4.0 mmol), pyridine (2.4 g, 30 mmol), and DMAP (catalytic amount) in CH_2Cl_2 (20 mL) was stirred at room temperature for 120 h. The reaction mixture was poured into water and extracted with chloroform (3 times). The organic layers were washed with water (2 times), 0.5 N HCl solution (2 times), and brine, and the solvent was evaporated. Pure acid was obtained by a single crystallization from CH_2Cl_2:hexane (4:1) in an 80% yield. ^{1}H NMR ($CDCl_3$): δ 9.43−8.33 (m, 5H, CH aromatic: *Z*/*E* isomers); 4.63 (t, 2H, CH_2ON); 4.08 (t, 2H, CO_2CH_2); 2.64, 2.66 (2 × t, 2 × 2H, succinic acid); 1.96, 1.95, 1.60−1.20 (m, 9 × 2H, spacer). The intermediate product (0.25 g, 0.42 mmol), **D1** (0.32 g, 0.42 mmol), dicyclohexylcarbodiimide (DCC) (2.1 g, 1.0 mmol), and DMAP (catalytic amount) were stirred in CH_2Cl_2 (15 mL) for 40 h at room temperature. The reaction mixture was diluted with CH_2Cl_2, washed with water (2 times), 0.5 N HCl solution (2 times) and brine (1 time), and dried over $MgSO_4$, and the solvent was evaporated. After drying in vacuo, the product was purified by column chromatography (SiO_2, eluent CH_2Cl_2), yielding a yellow-orange solid in a 33% yield. ^{1}H NMR ($CDCl_3$): δ 9.21−8.01 (m, 5H, CH fluorene, *Z*/*E* isomers); 7.52, 7,37 (2 × m, 10 + 15H, CH phenyl); 4.37 (t, 2H, CH_2ON); 4.26 (t, 2H, CH_2OPh); 4.08, 4.09 (2 × t, 2 × 2H, CO_2CH_2); 2.64, 2.63 (s, 4H, succinic acid); 1.92−1.20 (m, 18 × 2H, spacer).

Poly[11-(pentakis(phenylethynyl)phenoxy))undecyl acrylate-*co*-11-((*Z*,*E*)-2,4,7-trinitro-9-fluorenylideneaminooxy)undecyl acrylate-*co*-methyl acrylate] (P(DA)). The polymer was prepared from PAC and an equimolar mixture of **D1** and **A1**, using the procedure described for **P(D1)**. The second precipitation from chloroform into methanol yields a yellow-orange powder. The degree of substitution was determined to be 39% for both substituents; yield 0.98 mg, 94%. ^{1}H NMR ($CDCl_3$): δ 7.6−9.1 (CH fluorene); 7.1−7.5 (CH aromatic phenyls); 4.1, 4.2 (CH_2O ends of the spacer); 3.7 (OCH_3 methyl acrylate); 1.1−2.5 (CH_2, CH aliphatic spacer and backbone).

Charge-Transfer Complexes. Charge-transfer (CT) complexes were prepared by dissolving the appropriate amounts of donor and acceptor in a common solvent (CH_2Cl_2, $CHCl_3$, or *o*-$C_6H_4Cl_2$ for the two-polymer mixture). Evaporation of the solvent and drying for 24 h in vacuo yielded the strongly colored complexes.

Results

Synthesis. The synthesis of the investigated compounds is presented in Scheme 1. Preparation of **D1**, employing a 5-fold palladium-catalyzed cross-coupling[9] between a terminal acetylene and a pentabromophenol derivative, is well described in the literature.[8] 2,4,7-Trinitro-9-fluorenone (**A2**) was functionalized by an

Table 1. Thermal Behavior of the Pure Compounds; Transition Temperatures Are Given in °C and Latent Heat (in Parentheses) in J g^{-1}

material	thermal behavior[a]		
D1	K	122 (39)	I
P(D1)	G_I	53	I
A1	K	98−109 (54)	I
A2	K	176 (59)	I
A3	K	276 (78)	I
P(A1)	G_I	50	I

[a] K = crystalline; G = glassy; I = isotropic.

acid-catalyzed oxime exchange reaction with an 11-hydroxyuncedyl oxime derivative in glacial acetic acid,[10] followed by a saponification of the formed acetyl group at the terminal end of the spacer, yielding **A1**. Reaction of **A1** with succinic anhydride yielded a carboxylic acid functionalized TNF derivative that was esterified with **D1** to obtain the asymmetric twin **DA** with an analogous spacer length.[11]

The polymers **P(D1)**, **P(A1)**, and **P(DA)** were prepared by a nucleophilic substitution reaction on the reactive poly(acryloyl chloride) (PAC),[12] since their corresponding monomers were unwilling to polymerize under various conditions.[3i] To prepare **P(D1)**, **P(A1)**, and **P(DA)**, a solution of PAC, prepared by polymerization under standard free radical conditions, was simply added to the monomers **D1** and/or **A1** under normal esterification conditions. To prevent the formation of carboxylic acid groups, which are expected to have a large impact on the stability and the thermal properties, methanol was added at the final stages of the reaction. The copolymer **P(DA)** reflected an equal degree of substitution of both the donor and the acceptor, indicating matching reactivities of both hydroxyl groups. For all polymers, a degree of substitution between 70 and 80% was calculated from the relative intensities in the ^{1}H NMR spectra.

The thermal results of the pure materials are summarized in Table 1. The low molar mass compounds are crystalline solids, and the polymers are amorphous materials. None of the pure donors or acceptors showed liquid crystalline behavior.

Charge-Transfer Complexes. Initially, studies on the thermal properties of CT complexes of **D1**:**A2** and **P(D1)**:**A2** as a function of acceptor concentration were performed. In addition to multiple mixtures that were analyzed by DSC and OPM, contact samples of the donors with **A2** were analyzed with OPM. This resulted in simplified phase diagrams, as depicted in Figure 3. From the diagrams, it is evident that at equimolar ratios the best properties are found, i.e., absence of biphasic regions and a maximum in the transition temperatures. Deviation from the 1:1 ratio results in the formation of distinct biphases. For this reason, only equimolar complexes have been investigated in more detail. Optimal properties at 1:1 ratios have been reported for similar materials before;[6] however, it is not always the case since other optimal ratios have been reported for different CT complexes.[7b,c]

The thermal properties of the equimolar CT complexes were studied by OPM and DSC. They are summarized in Table 2. Some examples of DSC traces, all second heating, are depicted in Figure 4. All materials showed reproducible DSC results. Complexes with **A3** (not shown) exhibit dissimilar second heating runs, since substantial thermal degradation was observed during the first heating.

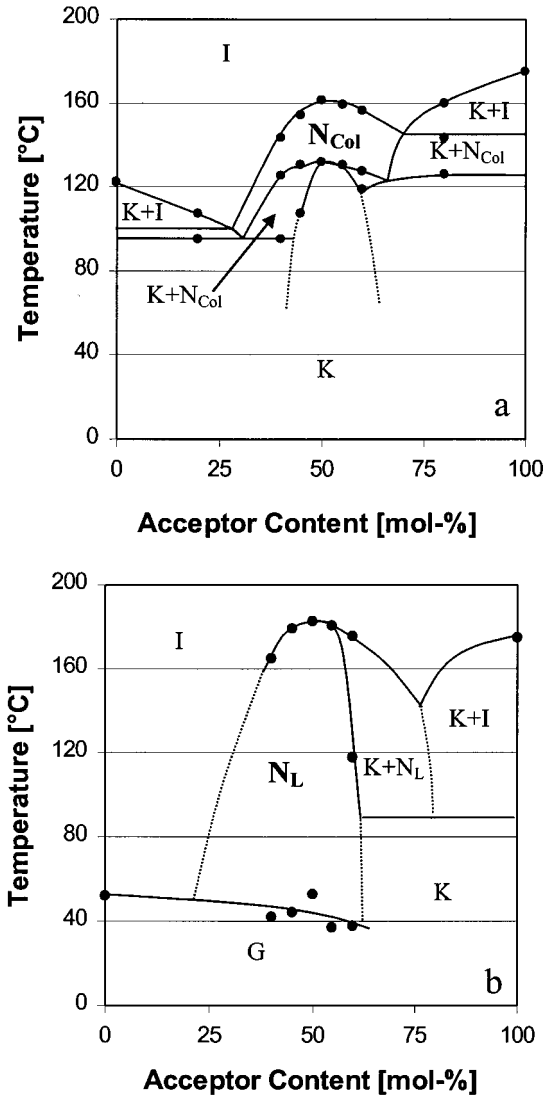

Figure 3. Simplified phase diagrams of (a) **D1**:**A2** and (b) **P(D1)**:**A2**.

The CT complexes of **D1** and **P(D1)** with **A1** and **P(A1)** and their intramolecular analogues all possessed nematic mesophases. Low molar mass complexes **D1**:**A1** and **DA** crystallized upon cooling, whereas the macromolecular complexes showed a glass transition and their optical textures were frozen in. Except for **DA**, the clearing temperatures were close to each other. Only the latent heat values at the N to I transitions, roughly corresponding to the extent of order in the nematic phase, varied considerably. The transition temperatures and latent heat values of **P(D1)**:**P(A1)** were measured after annealing for 10 h at 100 °C.

Complexing **D1** and **P(D1)** with electron acceptors **A2** and **A3** resulted in liquid crystalline materials at equimolar concentrations as well. The observed phases (nematic as well as columnar) and transition temperatures (T_i ranging from 90 to >250 °C) were strongly dependent on the acceptor. Again, incorporation of **D1** in a polymer fully suppressed crystallization, whereas the clearing points did not change much. For **P(D1)**:**A2** a strong increase in the latent heat at the N to I transition was observed as compared to the equivalent **D1**:**A2**. Complex **P(D1)**:**A3** revealed a columnar texture in microscopy studies, although no transitions were found before degradation started at high temperatures.

Table 2. Thermal Behavior of Equimolar Complexes of D1 and P(D1) with a Series of Electron Acceptors A1−A3 and P(A1) Measured with OPM and DSC; Transition Temperatures Are Given in °C and Latent Heat (in Parentheses) in J g^{-1}

complex				**D1**					**P(D1)**	
A1	K	93 (20)	N_D	96 (1.2)	I	G_{N_L}	33	N_L	101 (5)	I
P(A1)	G_{N_L}	28	N_L	103 (5)	I	$G_{N_{Col}}$	65	N_{Col}	94 (3)	I
A1	K	93 (20)	N_D	96 (1.2)	I	G_{N_L}	28	N_L	103 (5)	I
A2	K	132 (39)	N_{Col}	161 (1)	I	G_{N_L}	50	N_L	164 (5)	I
A3	K	200 (10)	Col_h	227 (12)	I	G_{Colh}	50	Col_h	>250	d
				Intramolecular CT Complexes						
DA	K	32 (1)				N_D	84 (1)	I		
P(DA)	$G_{N_{Col}}$	80				N_{Col}	104 (5)	I		

[a] K = crystalline; $G_{(M)}$ = glassy (mesophase frozen in); N_D = nematic discotic; N_L = nematic lateral; N_{Col} = nematic columnar; Col_h = columnar hexagonal; I = isotropic; d = decomposition.

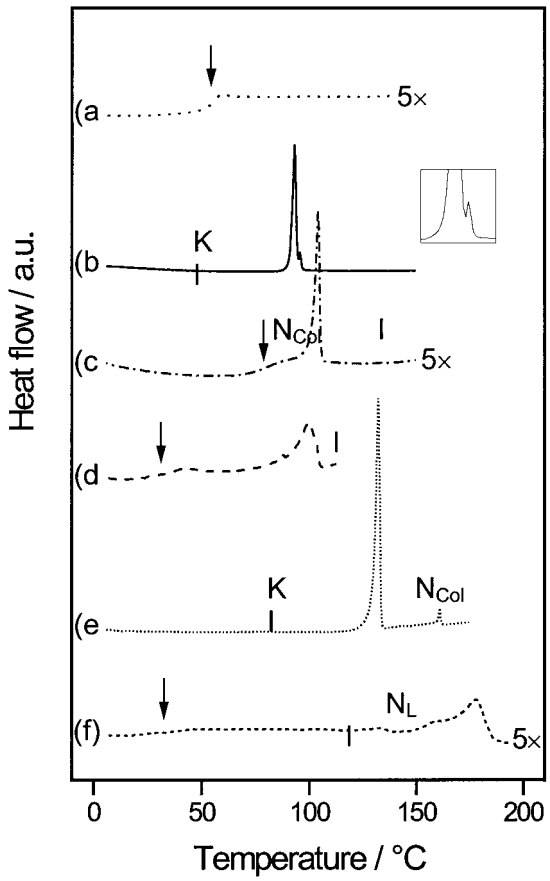

Figure 4. Normalized DSC traces of (a) **P(D1)** and various CT complexes: (b) **D1**:**A1** (with magnification of the small N_D phase in the frame), (c) **P(DA)**, (d) **P(D1)**:**A1**, (e) **D1**:**A2**, and (f) **P(D1)**:**A2**. The arrows indicate the glass transitions. Note that (a), (c), (d), and (f) are magnified 5× to for reasons of clarity.

Powder X-ray Diffraction. We have described detailed X-ray diffraction (XRD) analysis of complexes **D1**:**A1** and **D1**:**P(A1)**.[4c] The low molar mass complex showed a typical N_D pattern with just diffuse reflections, whereas the one-polymer complex showed the pattern of the newly identified N_L phase, i.e., much sharper reflections in the columnar and lateral direction as well as a clearly visible (100) reflection at small angles. The opposite **P(D1)**:**A1** complex showed an nearly identical pattern. Also, the polymer mixture **P(D1)**:**P(A1)** as well as the copolymer **P(DA)** exhibited sharp reflections at large angles (i.e., columnar direction), though their small-angle reflections were much more diffuse. CT complexes with **A3** showed further peak narrowing, as would be expected for columnar phases. In Figure 5 the XRD patterns of the observed liquid crystalline phases are presented.

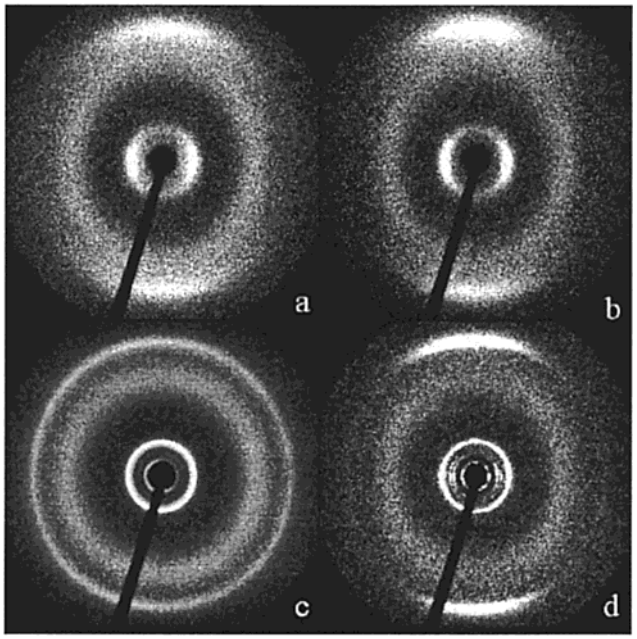

Figure 5. XRD patterns of observed mesophases a: (a) N_D phase (**D1**:**A1** at 90 °C), (b) N_{Col} phase (**D1**:**A2** at 150 °C), (c) N_L phase (**D1**:**P(A1)** at 90 °C), and (d) Col_h phase (**D1**:**A3** at 210 °C). Maximum diffraction angle: $2\theta = 30°$.

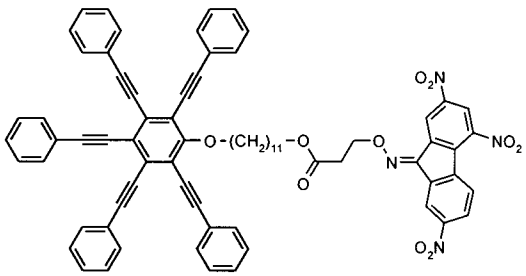

Figure 6. Asymmetric donor−acceptor twin investigated by Janietz.

For a more quantitative analysis, the spacings d were calculated using the Bragg law: $2d \sin\theta = n\lambda$, where θ is the diffraction angle and λ the wavelength (1.54 Å). Relatively low ordered materials, typically liquid crystals, show a periodic density wave with an exponential decay of the form $\rho(z) \propto \cos(kz)e^{-z/\xi}$, where k is the reciprocal lattice constant and ξ is the correlation length, a length scale of spatial order. This results in a Lorentzian distribution of the reflections, from which ξ can be calculated, using

$$\xi = \frac{2\pi}{q_{HW} - q_0} = \frac{\lambda/2}{\sin(\theta_{HW}) - \sin(\theta_0)} = \frac{\lambda}{\omega_{1/2}\cos(\theta_0)}$$

Here q is the modulus of the scattering vector: $q \equiv |\mathbf{q}| = 4\pi \sin(\theta)/\lambda$, θ_0 is the diffraction angle at the maximum, θ_{HM} is the diffraction angle of the half-width of the reflection, and $\omega_{1/2}$ is the full width at half-maximum of the reflection peak, which is easily determined after fitting the X-ray patterns with Lorentzian profiles. To describe experimental results, often the Scherrer equation that includes an extra constant is used:

$$\xi = \frac{0.89\lambda}{\omega_{1/2}\cos(\theta_0)}$$

The correlation lengths ξ (expressed in angstroms) calculated by the Scherrer equation for the various spacings d are summarized in Tables 3 and 4.

Discussion

The CT complex **D1**:**A1** showed an induced nematic discotic phase in a very small temperature range. By changing one of the constituents into the high molecular weight material, the phase behavior changed dramatically. Crystallization was suppressed, and because of the plasticizing effect of the tail of **A1**, the glass transition of the complex dropped to room temperature. This resulted in an increased mesophase window from 3 to about 70 °C, since the N to I transition temperature remained nearly constant. The strong rise of the latent heat at the clearing temperature resulted from the increased order of the N_L phase. This is clearly demonstrated by the high correlation lengths in both the (200) and the (001) direction. The thermal data of **D1**:**P(A1)** and **P(D1)**:**A1** are nearly identical, indicating that it is of no importance which of the constituents, donor or acceptor, is bound to the polymer backbone.

The polymer mixture **P(D1)**:**P(A1)** is highly viscous, and hence, it was difficult to obtain a homogeneous mixture.[13] DSC experiments showed sharper transitions at higher temperatures for longer annealing times, indicating a continuing homogenization process, but on very long time scales. An annealed sample showed an increase in T_g and a slight decrease in T_i, accompanied by a decrease in the latent heat, as compared to the one-polymer complexes. In contrast to the polymer mixture, **P(DA)** was much easier to handle, and this is also indicated by the sharp transitions observed in the DSC trace (Figure 4). Thin films for microscopy experiments were obtained by simply shearing the polymer in the nematic phase between two glass slides. The latent heat at the clearing point is of the order of the one-polymer complexes, indicative of a N_L to I transition. However, for both **P(D1)**:**P(A1)** and **P(DA)**, powder X-ray diffraction measurements indicate a N_{Col} phase. The combined observation of a high correlation length in the (001) direction and a much lower correlation length in the (200) direction corresponds better to the N_{Col} phase by using the classification that we described before.[4c] Another argument in favor of a N_{Col} phase and opposing a N_L phase results from miscibility studies of the nematic phase of **P(DA)** with the N_L phases of **P(D1)**:**A1** or **D1**:**P(A1)**. Although miscibility would be expected on the basis of the resembling molecular structures and other miscibility studies (e.g., the N_L phases of **P(D1)**:**A1** and **D1**:**P(A1)** are perfectly miscible), contact samples clearly show that both nematic phases are not miscible. Taking into account all our experimental data, we conclude that for both fully macromolecular CT complexes a N_{Col} phase is most likely.

Table 3. XRD Results of High and Low Molar Mass CT Complexes

complex	T [°C]	phase	Miller indices	d [Å]	ξ [Å]	ξ/d
			200	13.4	59	4.4
D1:**A1**	95	N_D	alkyl	4.8	23	4.8
			001	3.56	36	10
			200	12.6	212	17
D1:**P(A1)**	90	N_L	alkyl	4.7	26	5.5
			001	3.57	61	17
			200	12.8	242	19
P(D1):**A1**	90	N_L	alkyl	4.8	26	5.4
			001	3.52	63	18
			200	13.1	100	7.7
P(D1):**P(A1)**	90	N_{Col}	alkyl	4.9	31	6.5
			001	3.58	58	16
			200	13.0	106	8.2
P(DA)	90	N_{Col}	alkyl	4.8	24	5.0
			001	3.57	59	16

Table 4. XRD Results of CT Complexes with an Increasing Donor−Acceptor Interaction Strength

complex	T [°C]	phase	Miller indices	d [Å]	ξ [Å]	ξ/d
			200	13.5	82	6.0
D1:**A2**	150	N_{Col}	alkyl	4.9	22	4.5
			001	3.53	60	17
			200	12.7	179	14
P(D1):**A2**	150	N_L	alkyl	4.8	22	4.6
			001	3.52	43	12
			200	13.0	308	24
D1:**A3**	210	Col_h	alkyl	5.0	21	4.1
			001	3.48	134	38
			200	12.6	261	21
P(D1):**A3**	200	Col_h	alkyl	5.0	29	5.8
			001	3.54	80	23

Complexing **D1** and **P(D1)** with the stronger acceptor **A2** resulted in a strong increase in the clearing temperature. The CT complex **D1**:**A2** was reported previously to exhibit a N_{Col} phase.[8] This result is confirmed by our XRD experiments. The macromolecular complex **P(D1)**:**A2** showed suppression of crystallization. From the high latent heat at the clearing point and the increased lateral ordering (in the (200) direction), the formation of a N_L phase is deduced. Moreover, contact samples of **P(D1)**:**A2** and **P(D1)**:**A1** show the formation of well-mixed areas at the interfaces.

Studies on the steric effect of the spacer in complexes very similar to **D1**:**A2** show that high ordered mesophases (Col_{ho}) are suppressed at sufficient spacer length ($>C_{11}$).[21] However, increasing the donor−acceptor interaction strength by employing **A3** gave rise to higher ordered columnar phases again. From this we can conclude that in **D1**:**A3** the CT interaction strength, which promotes highly ordered mesophases, dominates over the steric effects, which oppose high order. The columnar phases are easily identified by their characteristic optical textures and the XRD patterns with sharper reflections and hence higher correlation lengths. Where the low molar mass complex has a crystallization temperature of 200 °C, the polymer does not show any transition before decomposition starts at elevated temperatures. This is a clear example of the extension of

the temperature window of the mesophase to nearly 200 °C by using macromolecular compounds.

Conclusions

By means of a polymer analogous substitution reaction, we have synthesized a number of functional polymers, which were virtually impossible to prepare from the monomers under standard free-radical polymerization conditions. Using this versatile approach, various polymers with comparable molecular weights and degrees of substitution could be prepared.

Mixing the electron donors with electron acceptors resulted in the formation of charge-transfer complexes because of noncovalent interactions. At exact equimolar ratios of **D1** and **P(D1)** with **A2**, stable complexes were found that effectively act as a single mesogenic CT species. By incorporating the mesogens into various macromolecular structures and via variation of the strength of the CT complex, it was possible to obtain insight into the mechanisms that give rise to the mesophase formation.

In the low molecular weight complex the traditional N_D phase was induced. If only one of the species is a polymer, a novel N_L phase with increased lateral order was observed. Finally, fully polymeric systems formed N_{Col} phases with only columnar order. Interestingly, the corresponding asymmetric dimer **DA** showed a much lower clearing point, and hence, it is a remarkable exception in this series of materials. Therefore, it is not a good model compound for the polymer equivalent **P(DA)**, for which reason it was designed originally.

The effect of the donor−acceptor interaction strength was studied by a series of different substituted TNF-based acceptors. Complexing **D1** with a weak, intermediate, and a strong acceptor resulted in the formation of a N_D, N_{Col}, and a Col_h phase, respectively. A strong increase both of the melting temperature and the clearing temperature was found with increasing acceptor strength. When **D1** was substituted for **P(D1)**, a N_L phase and Col_h phase were obtained. In addition, suppression of crystallization led to the formation of a broad temperature window of liquid crystalline behavior.

Using only a limited amount of nonliquid crystalline materials, we have been able to prepare a number of complexes with a wide range of mesophases and transition temperatures. This clearly demonstrates versatility of noncovalent interactions, such as charge-transfer complexing. The liquid crystalline diversity expands even further when macromolecular species are applied. Often studies of (discotic) liquid crystalline polymers suffer from experimental problems, like slow developing textures that are hard to interpret, broad phase transitions, and high viscosities, which result in a complex and undefined phase behavior. However, now it is shown that polymers can be used to our benefit in exploring new (N_L) and uncommon (N_{Col}) mesophases.

Acknowledgment. Ben Norder is gratefully acknowledged for technical assistance with thermal measurements and Enno Klop of Akzo Nobel Chemicals Research Arnhem−Applied Physics Department for assistance in performing the XRD analysis.

References and Notes

(1) Chandrasekhar, S.; Sadashiva, B. K.; Suresh, K. A. *Pramana* **1977**, *9*, 471.

(2) (a) Cammidge, A. N.; Bushby, R. J. In *Handbook of Liquid Crystals*; Demus, D., Goodby, J. W., Gray, G. W., Spiess, H. W., Vill, V., Eds.; Wiley VCH: New York, 1998; Vol. 2B, pp 693−748. (b) Chandrasekhar, S. *Liq. Cryst.* **1993**, *14*, 3−14. (c) Chandrasekhar, S.; Ranganath, G. S. *Rep. Prog. Phys.* **1990**, *53*, 57−84. (d) Destrade, C.; Tinh, N. H.; Gasparoux, H.; Malthête, J.; Levelut, A. M. *Mol. Cryst. Liq. Cryst.* **1981**, *71*, 111−135.

(3) (a) Boden, N.; Bushby, R. J.; Cammidge, A. N.; Headdock, G. *J. Mater. Chem.* **1995**, *5*, 2275−2281. (b) Wenz, G. *Makrom. Chem., Rapid Commun.* **1985**, *6*, 577−584. (c) Herrmann-Schönherr, O.; Wendorff, J. H.; Kreuder, W.; Ringsdorf, H. *Makrom. Chem., Rapid Commun.* **1986**, *7*, 97−101. (d) Ringsdorf, H.; Wüstefeld, R.; Zerta, E.; Ebert, M.; Wendorff, J. H. *Angew. Chem., Int. Ed. Engl.* **1989**, *28*, 914−918. (e) Kreuder, W.; Ringsdorf, H. *Makrom. Chem., Rapid Commun.* **1983**, *4*, 807−815. (f) Boden, N.; Bushby, R. J.; Lu, Z. B. *Liq. Cryst.* **1998**, *25*, 47−58. (g) Weck, M.; Mohr, B.; Maughon, B. R.; Grubbs, R. H. *Macromolecules* **1997**, *30*, 6430−6437. (h) Stewart, D.; McHattie, G. S.; Imrie, C. T. *J. Mater. Chem.* **1998**, *8*, 47−51. (i) Kouwer, P. H. J.; Mijs, W. J.; Jager, W. F.; Picken, S. J. *Macromolecules* **2000**, *33*, 4336−4342. (j) Favre-Nicolin, C. D.; Lub, J. *Macromolecules* **1996**, *29*, 6143−6149. (k) Disch, S.; Finkelmann, H.; Ringsdorf, H.; Schuhmacher, P. *Macromolecules* **1995**, *28*, 2424−2428. (l) Braun, C. D.; Lub, J. *Liq. Cryst.* **1999**, *26*, 1501−1509.

(4) (a) Kouwer, P. H. J.; Gast, J.; Jager, W. F.; Mijs, W. J.; Picken, S. J. *Mol. Cryst. Liq. Cryst.* **2001**, *364*, 225−234. (b) Kouwer, P. H. J.; Mijs, W. J.; Jager, W. F.; Picken, S. J. *J. Am. Chem. Soc.* **2001**, *123*, 4645−4646. (c) Kouwer, P. H. J.; Jager, W. F.; Mijs, W. J.; Picken, S. J. *Macromolecules* **2001**, *34*, 7582−7584.

(5) Tinh, N. H.; Destrade, C.; Gasparoux, H. *Phys. Lett.* **1979**, *72A*, 25.

(6) Praefcke, K.; Singer, D.; Kohne, B.; Ebert, M.; Liebmann, A.; Wendorff, J. H. *Liq. Cryst.* **1991**, *10*, 147−159.

(7) (a) Praefcke, K.; Singer, D. In *Handbook of Liquid Crystals*; Demus, D., Goodby, J. W., Gray, G. W., Spiess, H. W., Vill, V., Eds.; Wiley VCH: New York, 1998; Vol. 2B, pp 945−967. (b) Ringsdorf, H.; Wüstefeld, R. *Philos. Trans. R. Soc. London* **1990**, *A330*, 95−108. (c) Praefcke, K.; Holbrey, J. D. *J. Inclusion Phenom.* **1996**, *24*, 19−41.

(8) Janietz, D.; Hofmann, D.; Reiche, J. *Thin Solid Films* **1994**, *244*, 794−798.

(9) (a) Sonogashira, K.; Tohda, Y.; Nagihara, N. *Tetrahedron Lett.* **1975**, 4467. (b) Brandsma, L.; Vasilevsky, S. F.; Verkuijsse, H. D. In *Applications of Transition Metal Catalysis in Organic Synthesis*; Springer-Verlag: Berlin, 1998; pp 198−225.

(10) Newman, M. S.; Lutz, W. B. *J. Am. Chem. Soc.* **1956**, *78*, 2469−2473.

(11) (a) Janietz, D. *Chem. Commun.* **1996**, 713−714. (b) Previously, other linked donor−acceptors twins were prepared by Janietz [ref 11a]. However, the spacer length in these materials was significantly shorter. This may explain the fact that he found a completely different mesophase behavior for a similar material (shown in Figure 6).

(12) Strohriegl, P. *Makromol. Chem.* **1993**, *194*, 363−387.

(13) A mixture of two polymers is hard to make due to immediate precipitation of the polymers when the two solutions are poured together. After removal of the solvent, the precipitate was annealed for several hours prior to the DSC measurement to allow optimal mixing of the two polymer materials.

MA011628C